Int. J. Heat Mass Transfer. Vol. 36, No. 7, pp. 1859–1866, 1993
Printed in Great Britain

0017–9310/93 $6.00+0.00

Laminar mixed convection over horizontal flat plates with power-law variation in surface temperature

W. R. RISBECK, T. S. CHEN and B. F. ARMALY
Department of Mechanical and Aerospace Engineering and Engineering Mechanics, University of Missouri-Rolla, Rolla, Missouri

(*Received* 3 *February* 1992 *and in final form* 25 *August* 1992)

Abstract—An analysis is performed to study the heat transfer characteristics of laminar mixed convective boundary-layer flow over a semi-infinite horizontal flat plate with non-uniform surface temperatures. The surface temperature is assumed to vary as a power of the axial coordinate measured from the leading edge of the plate. A nonsimilar mixed convection parameter χ and a pseudo-similarity variable η are introduced to cast the governing boundary layer equations and their boundary conditions into a system of dimensionless equations which are solved numerically by a weighted finite-difference method. The mixed convection parameter χ is chosen so that $\chi = 0$ corresponds to pure free convection and $\chi = 1$ corresponds to pure forced convection. Numerical results are presented for Prandtl numbers of 0.1, 0.7, 7 and 100 and representative values of the exponent n for the power-law variation in wall temperature. The heat transfer results are compared with existing correlations for the uniform wall temperature case and new correlations are derived for the general case of power-law wall temperature variations. It is found that an increase in the Prandtl number and exponent value n increases the local heat transfer rate.

INTRODUCTION

IN THE study of convective heat transfer it is customary to treat the problem as either pure forced convection or pure free convection. However, combined forced and free convection or 'mixed' convection arises in many transport processes in nature and in engineering devices (such as atmospheric boundary layer flows, heat exchangers, solar collectors, nuclear reactors, and electronic equipment) in which the effect of buoyancy forces on a forced flow, or the effect of forced flow on a buoyant flow, is significant. Mixed convection in laminar boundary layer flow has been extensively analyzed for vertical flat plates (see, for example [1–4]), inclined plates [5, 6] and horizontal flat plates [7–13]. Most past studies dealt with forced convection dominated regime, that is forced convection under the influence of relatively weak to moderately strong buoyancy forces.

In their analysis of the buoyancy force effect on forced convection over horizontal plates Mori [7] and Sparrow and Minkowycz [8] found $Gr_x/Re_x^{5/2}$ as the buoyancy force parameter. Their solutions were carried out by perturbation series through the first two terms, which limited the validity of their results to weak buoyancy force effects, $Gr_x/Re_x^{5/2} \ll 1$. Later, Chen *et al.* [10] used the second level nonsimilarity method to obtain results for $-0.03 \leqslant Gr_x/Re_x^{5/2} \leqslant 1$ and found that the previous results substantially overestimated the buoyancy force effects when $Gr_x/Re_x^{5/2} > 0.2$. Ramachandran *et al.* [11] studied mixed convection over a horizontal plate under uniform wall temperature for the entire mixed convection regime, from pure forced convection to pure free convection, by using the parameter $Gr_x/Re_x^{5/2}$ to analyze the effect of buoyancy force on forced convection and the parameter $Re_x^{5/2}/\mathrm{Gr}_x$ to analyze the effect of forced flow on free convection. In an attempt to cover the entire regime of mixed convection along vertical and horizontal plates, Raju *et al.* [12] proposed new mixed convection parameters that are valid from pure forced convection to pure free convection. For the case of a horizontal plate under uniform wall temperature, they used the new parameter $Re_x^5/(Re_x^5+Gr_x^2)$ which reduces to 0 for pure free convection and to 1 for pure forced convection. Their Nusselt number results are limited to a range of Prandtl numbers Pr from 0.1 to 10.

The purpose of this investigation is to analyze mixed convection flow over a horizontal flat plate using a single mixed convection parameter that covers the entire regime of mixed convection, from the pure forced convection limit to the pure free convection limit. In contrast to the uniform wall temperature case treated by Raju *et al.* [12], in the present study the wall temperature of the plate is assumed to be non-isothermal and has a power-law variation with the axial coordinate. In addition, a different mixed convection parameter is employed, and results are given for $0.1 \leqslant Pr \leqslant 100$. Representative velocity and temperature profiles, and local wall shear stress and local Nusselt number results are presented. Correlation equations for the local and average Nusselt numbers are also developed for use in practical applications.

ANALYSIS

Consider laminar mixed convection flow over a semi-infinite horizontal flat plate with the wall temperature varying as $T_w(x) = T_\infty + ax^n$, where a and n are real constants. The free stream temperature is T_∞

NOMENCLATURE

f	reduced stream function, $\psi\chi/[\nu Re_x^{1/2}]$
g	gravitational acceleration
Gr_x	local Grashof number, $g\beta[T_w(x)-T_\infty]x^3/\nu^2$
Gr_L	Grashof number based on L, $g\beta[T_w(L)-T_\infty]L^3/\nu^2$
h	local heat transfer coefficient, $q_w/(T_w-T_\infty)$
$\bar{h}$	average heat transfer coefficient over length L
k	thermal conductivity of the fluid
L	an arbitrary length along the plate
n	exponent in the power law variation of the surface temperature
Nu_x	local Nusselt number, hx/k
$\overline{Nu}_L$	average Nusselt number, $\bar{h}L/k$
Pr	Prandtl number of the fluid, ν/α
Re_x	local Reynolds number, $u_\infty x/\nu$
Re_L	Reynolds number based on L, $u_\infty L/\nu$
T	fluid temperature
u	streamwise velocity component
v	normal velocity component
x	axial coordinate
y	normal coordinate.

Greek symbols

α	thermal diffusivity of fluid
β	volumetric coefficient of thermal expansion
η	pseudo-similarity variable $(y/x)Re_x^{1/2}\chi^{-1}$
θ	dimensionless temperature $(T-T_\infty)/[T_w(x)-T_\infty]$
ν	kinematic viscosity of the fluid
ρ	density of the fluid
τ_w	local wall shear stress
χ	mixed convection parameter, $Re_x^{1/2}/(Re_x^{1/2}+Gr_x^{1/5})$
ψ	stream function.

Subscripts

w	condition at the wall
∞	condition at the free stream
F	forced convection
N	natural convection.

Superscripts

$'$	denotes partial differentiation with respect to η.

and the free stream velocity parallel to the plate is u_∞. The x coordinate is measured from the leading edge of the plate and the y coordinate is measured normal to the plate. The corresponding velocity components in the x and y directions are u and v, respectively. Under the Boussinesq approximation, the governing boundary layer equations for a constant-property fluid may be written as [10]

$$\frac{\partial u}{\partial x}+\frac{\partial v}{\partial y}=0 \tag{1}$$

$$u\frac{\partial u}{\partial x}+v\frac{\partial u}{\partial y}=\pm g\beta\frac{\partial}{\partial x}\int_y^\infty (T-T_\infty)\,dy+\nu\frac{\partial^2 u}{\partial y^2} \tag{2}$$

$$u\frac{\partial T}{\partial x}+v\frac{\partial T}{\partial y}=\alpha\frac{\partial^2 T}{\partial y^2}. \tag{3}$$

The corresponding boundary conditions are

$$u=v=0,\quad T=T_w(x)=T_\infty+ax^n \quad \text{at } y=0$$
$$u\to u_\infty,\quad T\to T_\infty \quad \text{as } y\to\infty. \tag{4}$$

The first term on the right-hand-side of equation (2) is the buoyancy-induced streamwise pressure gradient and the plus and minus signs refer, respectively, to flow above and below the plate.

Next, the system of equations (1)–(4) can be transformed into a dimensionless form by introducing the following nondimensional quantities

$$\eta=\frac{y}{x}Re_x^{1/2}\chi^{-1},\quad \chi=\frac{Re_x^{1/2}}{Re_x^{1/2}+Gr_x^{1/5}} \tag{5}$$

$$f(x,\eta)=\frac{\psi}{\nu\,Re_x^{1/2}\chi},\quad \theta(\chi,\eta)=\frac{T-T_\infty}{T_w(x)-T_\infty} \tag{6}$$

where χ is the nonsimilar mixed convection parameter, with $Re_x=u_\infty x/\nu$ and $Gr_x=g\beta[T_w(x)-T_\infty]x^3/\nu^2$ denoting, respectively, the local Reynolds and Grashof numbers, η is a pseudo-similarity variable, $f(\chi,\eta)$ is the reduced stream function, and $\theta(\chi,\eta)$ is the dimensionless temperature. The stream function $\psi(x,y)$ satisfies the continuity equation with $u=\partial\psi/\partial y$ and $v=-\partial\psi/\partial x$. It is noted that the mixed convection parameter χ varies from 0 for pure free convection to 1 for pure forced convection.

The transformation yields:

$$f'''+\frac{1}{10}[5+(2n+1)(1-\chi)]ff''-\frac{(2n+1)}{5}(1-\chi)f'^2$$
$$\pm\frac{1}{10}(1-\chi)^5\Big\{[5-(2n+1)(1-\chi)]\eta\theta$$
$$+[5(2n+1)-(2n+1)(1-\chi)]\int_\eta^\infty\theta(\chi,\eta)\,d\eta$$
$$-(2n+1)\chi(1-\chi)\frac{\partial}{\partial\chi}\int_\eta^\infty\theta(\chi,\eta)\,d\eta\Big\}$$
$$=\frac{2n+1}{10}\chi(1-\chi)\left\{f''\frac{\partial f}{\partial\chi}-f'\frac{\partial f'}{\partial\chi}\right\} \tag{7}$$

$$\frac{\theta''}{Pr}+\frac{1}{10}[5+(2n+1)(1-\chi)]f\theta'-nf'\theta$$
$$=\frac{2n+1}{10}\chi(1-\chi)\left\{\theta'\frac{\partial f}{\partial\chi}-f'\frac{\partial\theta}{\partial\chi}\right\} \quad (8)$$

$$f'(\chi,0)=0,\quad f'(\chi,\infty)=\chi^2$$

$$[5+(2n+1)(1-\chi)]f(\chi,0)$$
$$-(2n+1)\chi(1-\chi)\frac{\partial f}{\partial\chi}(\chi,0)=0$$

$$\theta(\chi,0)=1,\quad \theta(\chi,\infty)=0. \quad (9)$$

In equations (7)–(9) the primes denote partial differentiation with respect to η and Pr is the Prandtl number. The plus/minus sign in front of the fourth term in equation (7) now stands for buoyancy assisting/opposing flow.

The system of equations (7)–(9) can be solved by an appropriate numerical scheme. However, it is much more convenient to do so by defining a new variable $G(\chi,\eta)$

$$G(\chi,\eta)=\int_\eta^\infty \theta(\chi,\eta)\,d\eta \quad (10)$$

such that

$$G'+\theta=0,\quad G(\chi,\infty)=0. \quad (11)$$

Equation (7) can then be written as

$$f'''+\frac{1}{10}[5+(2n+1)(1-\chi)]ff''-\frac{(2n+1)}{5}(1-\chi)f'^2$$
$$\pm\frac{1}{10}(1-\chi)^5\left\{[5-(2n+1)(1-\chi)]\eta\theta\right.$$
$$+[5(2n+1)-(2n+1)(1-\chi)]G$$
$$\left.-(2n+1)\chi(1-\chi)\frac{\partial G}{\partial\chi}\right\}$$
$$=\frac{2n+1}{10}\chi(1-\chi)\left\{f''\frac{\partial f}{\partial\chi}-f'\frac{\partial f'}{\partial\chi}\right\}. \quad (12)$$

Equations (8), (9), (11) and (12) comprise a system of equations that are coupled and they must be solved simultaneously. It is noted that for $\chi=0$ (pure free convection) and $\chi=1$ (pure forced convection) the f and θ equations reduce to ordinary differential equations and the boundary layers become similar.

The physical quantities of interest include the axial velocity distribution u, the temperature profile $\theta(\chi,\eta)$, the local Nusselt number $Nu_x=hx/k$, where $h=q_w/(T_w-T_\infty)$, with $q_w=-k(\partial T/\partial y)_{y=0}$ denoting the local surface heat flux, and the local wall shear stress $\tau_w=\mu(\partial u/\partial y)_{y=0}$. In terms of the transformation variables, the expressions for u/u_∞, Nu_x, and τ_w can be written as

$$u/u_\infty=f'(\chi,\eta)/\chi^2 \quad (13)$$

$$\frac{Nu_x}{Re_x^{1/2}+Gr_x^{1/5}}=-\theta'(\chi,0) \quad (14)$$

and

$$\frac{\tau_w(x^2/\mu v)}{(Re_x^{1/2}+Gr_x^{1/5})^3}=f''(\chi,0). \quad (15)$$

Also of interest is the average Nusselt number $\overline{Nu}_L$ defined as $\overline{Nu}_L=\bar{h}L/k$, where $\bar{h}$ is the average heat transfer coefficient over the plate length L. By finding h from equation (14) and evaluating $\bar{h}$, along with the definition of χ, one can find

$$\frac{\overline{Nu}_L}{Re_L^{1/2}+Gr_L^{1/5}}=\frac{10}{2n+1}\chi_L\left\{\frac{\chi_L}{1-\chi_L}\right\}^{5/(2n+1)}$$
$$\times\int_{\chi_L}^1\frac{[-\theta'(\chi,0)]}{\chi^3}\left\{\frac{1-\chi}{\chi}\right\}^{(4-2n)/(2n+1)}d\chi \quad (16)$$

where Re_L, Gr_L and χ_L are Re_x, Gr_x and χ at $\chi=L$. The corresponding $\overline{Nu}_L$ expression for $\chi_L=0$ (pure free convection with $Re_L=0$) can be found as

$$\left(\frac{\overline{Nu}_L}{Re_L^{1/2}+Gr_L^{1/5}}\right)_{\chi_L\to0}=-\frac{5}{n+3}\theta'(0,0) \quad (17)$$

and the $\overline{Nu}_L$ expression for $\chi_L=1$ (pure forced convection with $Gr_L=0$) has the form

$$\left(\frac{\overline{Nu}_L}{Re_L^{1/2}+Gr_L^{1/5}}\right)_{\chi_L\to1}=-2\theta'(1,0). \quad (18)$$

NUMERICAL METHOD OF SOLUTION

Equations (8), (9), (11) and (12) constitute a system of nonlinear partial differential equations which were transformed into a system of first order nonlinear differential equations. These first order equations were expressed in finite-difference form by linearizing the nonlinear terms and using a weighted finite-difference method, as outlined in Lee *et al.* [14]. The resulting system of weighted finite-difference equations was then expressed in a matrix form and solved using a Gaussian elimination method. The solution provided f, f', and θ, and the cubic spline technique was employed to obtain f'' and θ'. A solution was considered to be converged if the newly calculated values for f, f' and θ differed from their previous guessed values within a tolerance of $\varepsilon\leqslant10^{-5}$. Successive guesses for new values of f, f' and θ were found from their calculated values and the previous guesses by the relationship $f_{new}=\omega f+(1-\omega)f_{old}$, etc. where ω is the relaxation factor. It is noted that underrelaxation ($\omega<1$) was rarely required for obtaining converged solutions.

The numerical results were found to depend upon η_∞ and the step size $\Delta\eta$. A step size of $\Delta\eta=0.02$ gave sufficient accuracy for Prandtl numbers of 0.1 through 7. However, a step size of $\Delta\eta=0.01$ was required for a Prandtl number equal to 100. The value of η_∞ was

chosen as large as possible between 10 and 20 without causing numerical oscillations in the values of f', θ, f'', and θ'. The choice of a step size of $\Delta\chi = 0.05$ was sufficient for all the cases considered. This indicated that $\Delta\chi$ is not so critical to the numerical accuracy as the choice of $\Delta\eta$ and η_∞.

RESULTS AND DISCUSSION

Numerical results were obtained for buoyancy-assisting flow covering Prandtl numbers of 0.1, 0.7, 7 and 100. The values of the mixed convection parameter χ ranged between 0 and 1, in increments of 0.05, and the values of the exponent n in $(T_w - T_\infty) = ax^n$ were taken as -0.4, 0, 1/3 and 1. This range of n values lies within the physical limits $-0.4 \leqslant n \leqslant 1$ as determined in a manner outlined by Gebhart [15].

Representative velocity distributions in terms of $(u/u_\infty)\chi^2 = f'(\chi, \eta)$ are presented in Figs. 1 and 2 for Prandtl numbers of 0.7 and 7. To conserve space, the velocity distributions for $Pr = 0.1$ and 100 are not shown. It is seen from these figures that the velocity profiles change from a predominantly forced convection profile (at $\chi = 1$) to that of the pure free convection profile (at $\chi = 0$). The effect of increasing the exponential value n for situations in which the influence of the buoyancy forces is significant (small χ values) is an apparent decrease in the maximum velocities inside the boundary layer for all the Prandtl numbers that were considered. The reasons for this trend can be explained as follows. In the vertical plate orientation the buoyancy force acts in the direction of the forced flow and therefore it will serve to aid the forced flow along the plate. For a horizontal plate the buoyancy force acts in the direction normal to the forced flow. When the exponent value n (and hence the wall-fluid temperature difference) increases, the buoyancy force normal to the plate will increase and act to retard the flow in the streamwise direction within the boundary layer under a strong buoyant flow (small χ value). For a weak buoyant flow (large χ value) the viscous forces are of greater significance and the change in the n value only slightly affects the velocity distribution in the boundary layer. Also, it is mentioned here that, in strong buoyant flow, as the Prandtl number increases, the effect of n on the velocity profiles is found to diminish and the peak value of $(u/u_\infty)\chi^2$ is found to decrease.

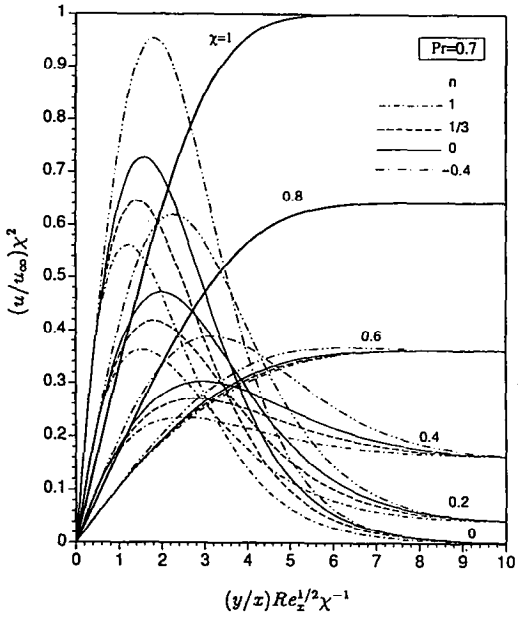

FIG. 1. Dimensionless velocity profiles, $Pr = 0.7$.

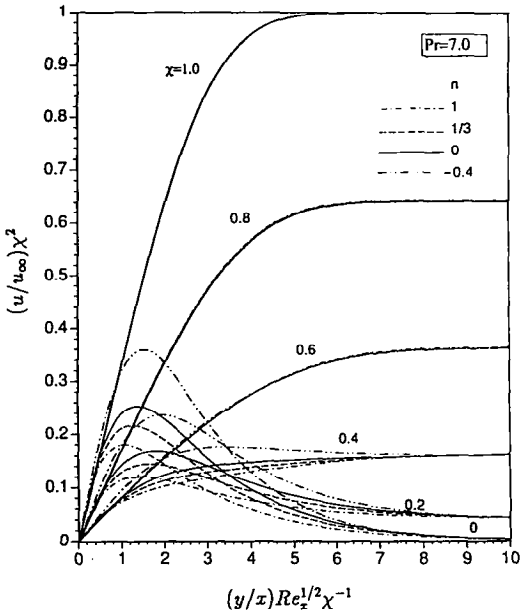

FIG. 2. Dimensionless velocity profiles, $Pr = 7.0$.

For a given power of n the value of χ at which a moderate to strong buoyancy force begins to affect the shape of the velocity profile is found to decrease as the Prandtl number increases. For $Pr = 0.1$ and 0.7 (Fig. 1) this occurs at approximately $\chi = 0.6$, where the profiles for larger powers of n dip below that of $n = 0$. For $Pr = 7$ (Fig. 2) and 100, significant changes in the shape of velocity profiles start to occur at $\chi = 0.4$ and $\chi = 0.2$, respectively. This behavior can be explained from the relative thickness between the momentum and thermal boundary layers. As χ decreases, the effect of buoyancy force increases. For low Prandtl numbers ($Pr < 1$) the thermal boundary layer thickness is larger than the momentum boundary layer thickness and the entire velocity field is affected by the temperature gradient. Thus the effect of buoyancy force on the velocity profiles can be felt at a smaller buoyancy force or at a larger value of χ. On the other hand, for high Prandtl numbers ($Pr \gg 1$) the momentum boundary layer thickness is much larger than the thermal boundary layer thickness and

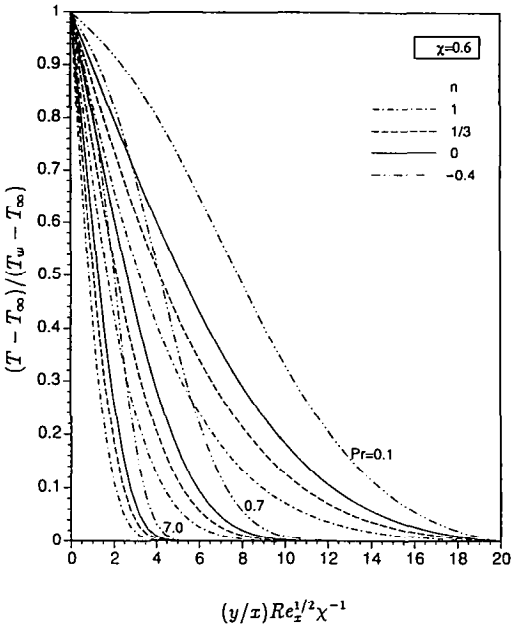

FIG. 3. Dimensionless temperature profiles, $\chi = 0.6$.

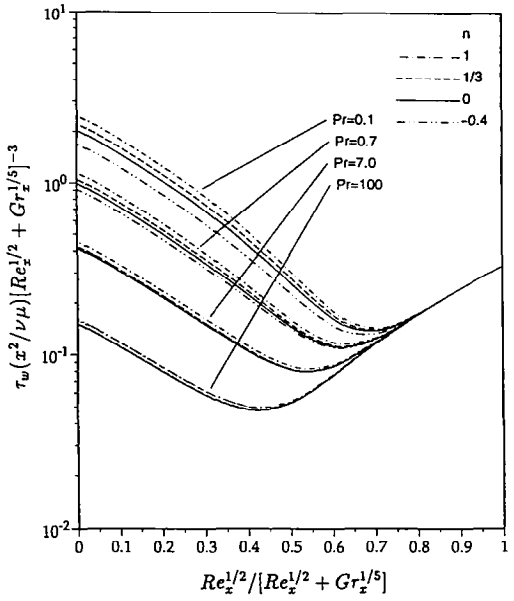

FIG. 5. Results for local wall shear stress $\tau_w(x^2/\mu v)(Re_x^{1/2}+Gr_x^{1/5})^{-3}$.

consequently the effect of buoyancy force induced by the fluid temperature gradient is localized in the region near the plate surface. This means that the effect of buoyancy force will not be significant until χ becomes small.

Representative temperature profiles are illustrated in Figs. 3 and 4 for $\chi = 0.6$ and 0.2. The temperature profiles for $\chi = 1.0$, 0.8, 0.4 and 0 are similar in shape to those for $\chi = 0.6$ and 0.2, and they are not illustrated. For a given value of χ it is found that the effect of either increasing the Prandtl number or increasing the exponent n is to increase the wall temperature gradient. Since an increase in the Prandtl number causes a relative decrease in the thermal boundary layer thickness one would expect the temperature gradient to increase. By increasing the value n, a larger heat flux can be expected at the wall, because the temperature gradient at the wall increases.

The local wall shear stress in terms of $\tau_w(x^2/\nu\mu)[Re_x^{1/2}+Gr_x^{1/5}]^{-3}$ and the local Nusselt number in terms of $Nu_x/[Re_x^{1/2}+Gr_x^{1/5}]$ as a function of $\chi = Re_x^{1/2}/[Re_x^{1/2}+Gr_x^{1/5}]$ are shown, respectively, in Figs. 5 and 6 for values of the exponent n of -0.4, 0, 1/3 and 1, and Prandtl numbers of $Pr = 0.1$, 0.7, 7.0

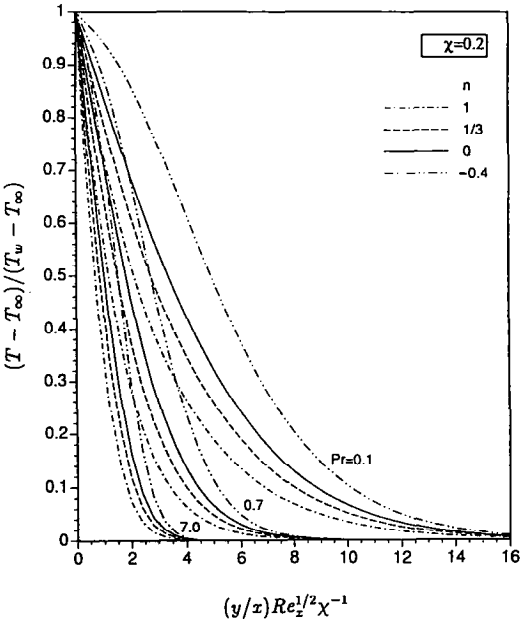

FIG. 4. Dimensionless temperature profiles, $\chi = 0.2$.

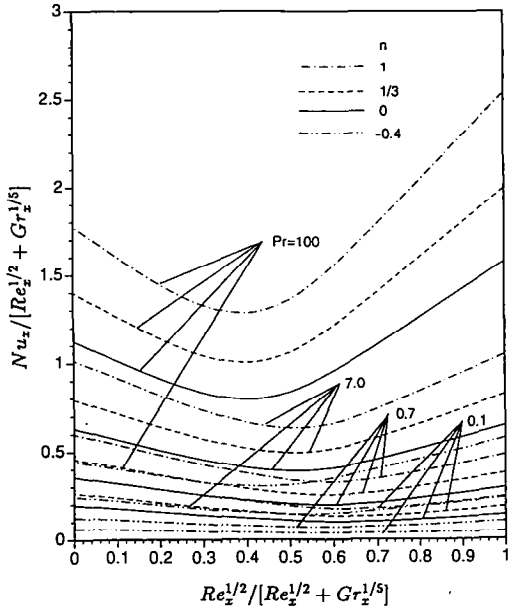

FIG. 6. Results for local Nusselt number $Nu_x/(Re_x^{1/2}+Gr_x^{1/5})$.

and 100. Their numerical values are also listed, respectively, in Tables 1 and 2. As can be seen from the figures, for a given n value, both the wall shear stress parameter and the surface heat transfer parameter initially decrease as χ increases from 0 until they reach a minimum value and thereafter increase as χ increases further to 1.0. These local minima occur at approximately $\chi = 0.7$, 0.6, 0.5 and 0.4 for Prandtl numbers of 0.1, 0.7, 7.0 and 100, respectively. The surface heat transfer rate, Fig. 6, increases with increasing n for a given value of χ, with higher heat transfer rates for larger Prandtl numbers. This is to be expected from the temperature profiles, Figs. 3 and 4. The wall shear stress, Fig. 5, also increases with increasing n for a given χ, with lower shear stress for a larger Prandtl number. The dependence of the wall shear stress on the Prandtl number can be explained by the fact that a smaller Prandtl number gives rise to a larger velocity gradient at the wall and hence a higher wall shear stress. The opposite is true for larger Prandtl numbers.

The behaviors of the local wall shear stress parameter $\tau_w(x^2/\nu\mu)[Re_x^{1/2}+Gr_x^{1/5}]^{-3}$ and the local Nusselt number parameter $Nu_x[Re_x^{1/2}+Gr_x^{1/5}]$, as seen in Figs. 5 and 6, seem to indicate a lower wall shear stress and Nusselt number for mixed convection than would be predicted for pure forced convection or pure free convection. However, this is not the case. For example, consider the case of $Pr = 0.7$, $n = 0$ and $\chi = 0.5$. If the Reynolds number is taken as $Re_x = 10^3$ the corresponding Grashof number can be found from the χ expression to be $Gr_x = 3.16 \times 10^7$. From Tables 1 and 2 (for $Pr = 0.7$ and $n = 0$) the local wall shear stress in terms of $\tau_w(x^2/\nu\mu)$ and the local Nusselt number Nu_x for the case of pure forced convection ($\chi = 1$, $Re_x = 10^3$, $Gr_x = 0$) are found to be 10 502 and 9.256, respectively. For the case of pure free convection ($\chi = 0$, $Gr_x = 3.16 \times 10^7$, $Re_x = 0$), the corresponding $\tau_w(x^2/\nu\mu)$ and Nu_x values are, respectively, 31 258 and 11.215. Next, from the mixed convection results for $\chi = 0.5$ (with $Re_x = 10^3$ and $Gr_x = 3.16 \times 10^7$), the local wall shear stress $\tau_w(x^2/\nu\mu)$ and the local Nusselt number Nu_x can be found to have the respective values 37 315 and 12.833. It is thus obvious that the predicted values of shear stress and Nusselt number for $\chi = 0.5$ (mixed convection) are actually higher than their respective values for pure forced convection and pure free convection.

The local Nusselt number Nu_x may alternately be expressed in terms of $Nu_x Re_x^{-1/2}$ as a function of $Gr_x Re_x^{-5/2}$. When these values are plotted using a log–log scale, as shown in Fig. 7, the resulting curves are typical of the results presented in previous studies where the mixed convective values are shown to asymptotically approach the straight lines for pure forced convection ($Gr_x/Re_x^{5/2} = 0$) and pure free convection ($Gr_x/Re_x^{5/2} \to \infty$). Again, the surface heat transfer rate is seen to increase with increasing n, with

Table 1. Results for the local wall shear stress $\tau_w(x^2/\mu\nu)(Re_x^{1/2}+Gr_x^{1/5})^{-3} = f''(\chi, 0)$

	$Pr = 0.1$				$Pr = 0.7$			
	n				n			
χ	−0.4	0	1/3	1	−0.4	0	1/3	1
0	1.6908	2.0296	2.2173	2.4794	0.9164	0.9889	1.0484	1.1453
0.1	1.2314	1.4777	1.6145	1.8056	0.6689	0.7212	0.7644	0.8346
0.2	0.8649	1.0358	1.1308	1.2633	0.4729	0.5081	0.5377	0.5859
0.3	0.5815	0.6928	0.7548	0.8405	0.3226	0.3443	0.3631	0.3938
0.4	0.3720	0.4387	0.4755	0.5256	0.2134	0.2251	0.2358	0.2535
0.5	0.2292	0.2645	0.2834	0.3085	0.1422	0.1475	0.1528	0.1617
0.6	0.1495	0.1648	0.1724	0.1825	0.1102	0.1125	0.1148	0.1187
0.7	0.1336	0.1383	0.1407	0.1438	0.1225	0.1237	0.1247	0.1263
0.8	0.1725	0.1737	0.1746	0.1756	0.1711	0.1720	0.1726	0.1734
0.9	0.2423	0.2429	0.2433	0.2437	0.2423	0.2428	0.2431	0.2436
1.0	0.3221	0.3321	0.3321	0.3321	0.3321	0.3321	0.3321	0.3321
	$Pr = 7.0$				$Pr = 100$			
	n				n			
χ	−0.4	0	1/3	1	−0.4	0	1/3	1
0	0.4262	0.4170	0.4288	0.4559	0.1611	0.1509	0.1526	0.1597
0.1	0.3116	0.3048	0.3133	0.3331	0.1180	0.1105	0.1118	0.1170
0.2	0.2216	0.2165	0.2224	0.2363	0.0850	0.0797	0.0806	0.0844
0.3	0.1539	0.1503	0.1542	0.1633	0.0620	0.0584	0.0591	0.0618
0.4	0.1073	0.1050	0.1074	0.1130	0.0499	0.0480	0.0486	0.0504
0.5	0.0826	0.0818	0.0832	0.0863	0.0527	0.0523	0.0529	0.0542
0.6	0.0850	0.0853	0.0862	0.0878	0.0748	0.0753	0.0759	0.0769
0.7	0.1167	0.1175	0.1181	0.1191	0.1146	0.1155	0.1161	0.1170
0.8	0.1705	0.1713	0.1718	0.1726	0.1703	0.1711	0.1716	0.1723
0.9	0.2422	0.2428	0.2431	0.2435	0.2422	0.2428	0.2431	0.2435
1.0	0.3221	0.3321	0.3321	0.3321	0.3321	0.3321	0.3321	0.3321

Table 2. Results for the local Nusselt number $Nu_x/(Re_x^{1/2}+Gr_x^{1/5}) = -\theta'(\chi, 0)$

	$Pr = 0.1$				$Pr = 0.7$			
			n				n	
χ	−0.4	0	1/3	1	−0.4	0	1/3	1
0	0.0620	0.1963	0.2619	0.3530	0.1244	0.3547	0.4580	0.5994
0.1	0.0560	0.1766	0.2356	0.3175	0.1121	0.3194	0.4123	0.5396
0.2	0.0504	0.1575	0.2098	0.2825	0.1003	0.2852	0.3680	0.4812
0.3	0.0453	0.1392	0.1851	0.2487	0.0892	0.2530	0.3261	0.4256
0.4	0.0413	0.1224	0.1623	0.2175	0.0793	0.2244	0.2888	0.3759
0.5	0.0383	0.1085	0.1435	0.1914	0.0717	0.2029	0.2608	0.3383
0.6	0.0364	0.1004	0.1322	0.1754	0.0685	0.1953	0.2509	0.3243
0.7	0.0355	0.1018	0.1338	0.1764	0.0726	0.2081	0.2671	0.3440
0.8	0.0372	0.1124	0.1476	0.1940	0.0817	0.2342	0.3002	0.3858
0.9	0.0408	0.1260	0.1654	0.2172	0.0918	0.2633	0.3372	0.4328
1.0	0.0451	0.1400	0.1837	0.2410	0.1021	0.2927	0.3745	0.4804
	$Pr = 7.0$				$Pr = 100$			
			n				n	
χ	−0.4	0	1/3	1	−0.4	0	1/3	1
0	0.2425	0.6303	0.7932	1.0145	0.4451	1.1239	1.4013	1.7760
0.1	0.2185	0.5676	0.7145	0.9139	0.4010	1.0130	1.2636	1.6022
0.2	0.1955	0.5079	0.6395	0.8183	0.3602	0.9114	1.1388	1.4465
0.3	0.1741	0.4535	0.5718	0.7323	0.3257	0.8305	1.0423	1.3289
0.4	0.1561	0.4101	0.5184	0.6645	0.3044	0.7933	1.0027	1.0847
0.5	0.1451	0.3885	0.4929	0.6323	0.3095	0.8321	1.0579	1.3564
0.6	0.1477	0.4037	0.5137	0.6582	0.3470	0.9486	1.2071	1.5450
0.7	0.1646	0.4536	0.5770	0.7378	0.4006	1.0987	1.3962	1.7836
0.8	0.1872	0.5163	0.6560	0.8374	0.4579	1.2559	1.5938	2.0331
0.9	0.2107	0.5811	0.7375	0.9404	0.5157	1.4139	1.7925	2.2840
1.0	0.2343	0.6460	0.8192	1.0437	0.5736	1.5720	1.9912	2.5349

higher transfer rates for larger Prandtl numbers, as was shown in Fig. 6.

Correlation equations for Nusselt numbers in forced convection are available for a wide range of Prandtl numbers and values of the exponent n. For pure forced convection the local and average Nusselt numbers for $0.1 \leqslant Pr \leqslant 100$ and $-0.4 \leqslant Pr \leqslant 0.5$ have been correlated by the following expressions [16]

$$Nu_{x,F}\, Re_x^{-1/2} = \alpha_F(Pr)[1 + V_F] \tag{19}$$

where

$$\alpha_F(Pr) = 0.339 Pr^{1/3}[1 + (0.0468/Pr)^{2/3}]^{-1/4} \tag{20}$$

$$V_F = n\{[1.17 + 11.0 \exp(-5.6 Pr^{1/10})] - 0.92n\} \tag{21}$$

and

$$\overline{Nu}_{L,F}\, Re_L^{-1/2} = 2\alpha_F(Pr)[1 + V_F]. \tag{22}$$

For pure free convection the local and average Nusselt numbers for $0.1 \leqslant Pr \leqslant 100$ and $-0.4 \leqslant n \leqslant 1.0$ from the present study can be correlated by the following expressions

$$Nu_{x,N}\, Gr_x^{-1/5} = \alpha_N(Pr)[1 + V_N] \tag{23}$$

where

$$\alpha_N(Pr) = (Pr/5)^{1/5} \frac{Pr^{1/2}}{(0.25 + 1.6 Pr^{1/2})} \tag{24}$$

as given by Chen *et al.* [17] and

$$V_N = n/A1 - n^2/A2 + n^3/A3 \tag{25}$$

with

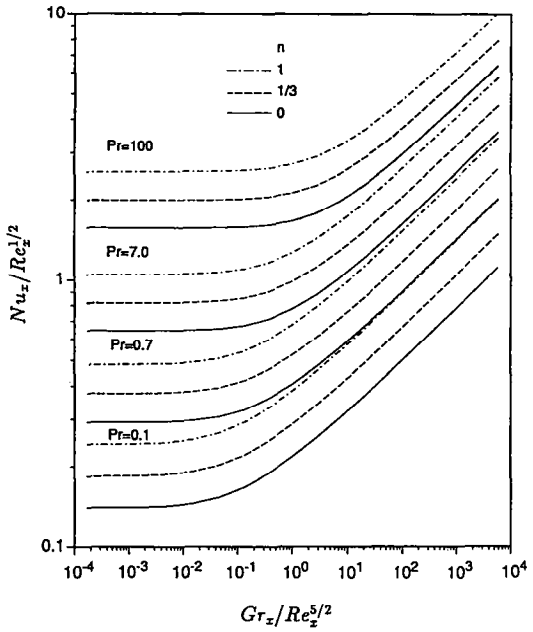

FIG. 7. $Nu_x\, Re_x^{-1/2}$ vs $Gr_x\, Re_x^{-5/2}$ for mixed convection.

$$A1 = 4.167 \times 10^{-2} \ln (Pr) + 0.9791$$

$$A2 = 5.450 \times 10^{-2} \ln (Pr) + 1.9990$$

$$A3 = 9.728 \times 10^{-2} \ln (Pr) + 5.9260. \quad (26)$$

The corresponding average Nusselt number has the expression

$$\overline{Nu}_{L,N} Gr_L^{-1/5} = \frac{5}{n+3} \alpha_N (Pr)[1 + V_N]. \quad (27)$$

The expression for V_N, equation (25), was developed using the results of this study to extend the correlation from $n = 0$ [16] to the general case of power-law wall temperature variation.

Following Churchill [18], the correlation equation for Nusselt numbers in mixed convection is expressed by the form

$$\left(\frac{Nu}{Nu_F}\right)^E = 1 + \left(\frac{Nu_N}{Nu_F}\right)^E. \quad (28)$$

This form of correlation has been found to give an accuracy of within 5% for $0.1 \leqslant Pr \leqslant 100$ for flat plates with $E = 3$. For the present study with a mixed convection parameter χ, the corresponding correlation equation for the mixed convection local Nusselt number can be represented by

$$\frac{Nu_x}{(Re_x^{1/2} + Gr_x^{1/5})} = \left\{\left[\chi\left(\frac{Nu_{x,F}}{Re_x^{1/2}}\right)\right]^E + \left[(1-\chi)\left(\frac{Nu_{x,N}}{Gr_x^{1/5}}\right)\right]^E\right\}^{1/E}. \quad (29)$$

It was found that the maximum difference between the correlated values from equation (29) and the calculated values is within 5% for $E = 3$.

The correlation equation for the mixed convection average Nusselt number can be similarly expressed by

$$\frac{\overline{Nu}_L}{(Re_L^{1/2} + Gr_L^{1/5})} = \left\{\left[\chi_L\left(\frac{\overline{Nu}_{L,F}}{Re_L^{1/2}}\right)\right]^E + \left[(1-\chi_L)\left(\frac{\overline{Nu}_{L,N}}{Gr_L^{1/5}}\right)\right]^E\right\}^{1/E}. \quad (30)$$

The maximum difference between the correlated values from equation (30) and the calculated values from equations (16)–(18) is found to be within 10% for $E = 3$.

CONCLUSIONS

In this paper, mixed convection in laminar boundary-layer flow over horizontal flat plates has been studied analytically for the case of power-law variation in the wall temperature. The major findings of this study are: (1) Both the local surface heat flux and the local wall shear stress increase with increasing value of the exponent n for a given Prandtl number Pr, and (2) for a given value of the exponent n, the local surface heat transfer rate increases but the local wall shear stress decreases with increasing Prandtl number. The correlation equations for the local and average Nusselt numbers provide results that agree well with the numerically predicted values.

REFERENCES

1. J. R. Lloyd and E. M. Sparrow, Combined forced and free-convection flow on vertical surfaces, *Int. J. Heat Mass Transfer* **13**, 434–438 (1970).
2. P. H. Oosthuizen and R. Hart, A numerical study of laminar combined convective flow over flat plates, *J. Heat Transfer* **95**, 60–63 (1973).
3. G. Wilkes, Combined forced and free convection flow on vertical surfaces, *Int. J. Heat Mass Transfer* **16**, 1958–1964 (1973).
4. N. Ramachandran, B. F. Armaly and T. S. Chen, Measurements and predictions of laminar mixed convection flow adjacent to a vertical surface, *J. Heat Transfer* **107**, 636–641 (1985).
5. A. Mucoglu and T. S. Chen, Mixed convection on inclined surfaces, *J. Heat Transfer* **101**, 422–426 (1979).
6. N. Ramachandran, B. F. Armaly and T. S. Chen, Measurements of laminar mixed-convection flow adjacent to an inclined surface, *J. Heat Transfer* **109**, 146–151 (1987).
7. Y. Mori, Buoyancy effects in forced laminar convection flow over a horizontal flat plate, *J. Heat Transfer* **83**, 479–482 (1961).
8. E. M. Sparrow and W. J. Minkowycz, Buoyancy effects on horizontal boundary layer flow and heat transfer, *Int. J. Heat Mass Transfer* **5**, 505–511 (1962).
9. C. A. Heiber, Mixed convection above a heated horizontal surface, *Int. J. Heat Mass Transfer* **16**, 769–785 (1973).
10. T. S. Chen, E. M. Sparrow and A. Mucoglu, Mixed convection in boundary layer flow on a horizontal plate, *J. Heat Transfer* **99**, 66–71 (1977).
11. N. Ramachandran, B. F. Armaly and T. S. Chen, Mixed convection over a horizontal plate, *J. Heat Transfer* **105**, 420–423 (1983).
12. M. S. Raju, X. Q. Liu and C. K. Law, A formulation of combined forced and free convection past horizontal and vertical surfaces, *Int. J. Heat Mass Transfer* **27**, 2215–2224 (1984).
13. W. Schneider and M. G. Wasel, Breakdown of the boundary-layer approximation for mixed convection above a horizontal plate, *Int. J. Heat Mass Transfer* **28**, 2307–2313 (1985).
14. S. L. Lee, T. S. Chen and B. F. Armaly, New finite difference solution methods for wave instability problems, *Numer. Heat Transfer* **10**, 1–8 (1986).
15. B. Gebhart, *Heat Transfer* (2nd Ed.). McGraw-Hill, New York (1971).
16. J. J. Heckel, T. S. Chen and B. F. Armaly, Mixed convection along slender vertical cylinders with variable surface temperature, *Int. J. Heat Mass Transfer* **32**, 1431–1442 (1989).
17. T. S. Chen, B. F. Armaly and N. Ramachandran, Correlations for laminar mixed convection flows on vertical, inclined and horizontal flat plates, *J. Heat Transfer* **108**, 835–840 (1986).
18. S. W. Churchill, A comprehensive correlating equation for laminar assisting, forced and free convection, *A.I.Ch.E. Jl* **23**, 10–16 (1977).